Ultraviolet Photoelectron Spectroscopy of *o*-, *m*-, and *p*-Halobenzyl Anions

Joseph B. Kim,[†] Paul G. Wenthold,[‡] and W. C. Lineberger*

JILA, University of Colorado and National Institute for Standards and Technology, Department of Chemistry and Biochemistry, University of Colorado, Boulder, Colorado 80309-0440

The 351 nm photoelectron spectra of the ortho, meta, and para isomers of the fluorobenzyl, chlorobenzyl, and bromobenzyl anions all exhibit resolved, analyzable vibrational structure. For a given isomer, the electron affinity increases with increasing halide atomic number, while for a given halogen substituent, the meta isomer has the largest electron affinity and the para isomer has the lowest. The electron affinities of the *o*-, *m*-, and *p*-fluorobenzyl radicals are found to be 1.091 ± 0.008, 1.173 ± 0.008, and 0.937 ± 0.008 eV, respectively, the electron affinities of the *o*-, *m*-, and *p*-chlorobenzyl radicals are 1.257 ± 0.008, 1.272 ± 0.008, and 1.174 ± 0.008 eV, respectively, and the electron affinities of *o*-, *m*-, and *p*-bromobenzyl radicals are 1.308 ± 0.008, 1.307 ± 0.008, and 1.229 ± 0.008 eV, respectively. Two vibrational progressions are present in all of the halobenzyl spectra, corresponding to the ring-deformation mode and either a ring stretching mode or the CH_2 bending mode. The measured electron affinities are used together with previously reported gas-phase acidities to derive the 298 K, methyl C−H bond energies for the corresponding halotoluenes. DH_{298}(C−H) for *o*-, *m*-, and *p*-fluorotoluenes are found to be 90.6, 88.8 ± 2.1, and 87.6 ± 2.1 kcal/mol, respectively, DH_{298}(C−H) for *o*-, *m*-, and *p*-chlorotoluenes are 89.0 ± 3.1, 89.8 ± 2.1, and 87.5 ± 2.1 kcal/mol, respectively, and DH_{298}(C−H) for *o*-, *m*-, and *p*-bromotoluenes are 90.2 ± 3.1, 90.1 ± 3.1, and 88.5 ± 3.1 kcal/mol, respectively.

Introduction

As one of the simplest aromatic free radicals, the benzyl radical has spawned numerous studies, both experimental and theoretical. The radical has been examined using corona discharge emission,[1] laser-induced fluorescence (LIF),[2−5] and infrared techniques,[6] and many of its spectroscopic properties are well established. The thermochemical properties, in particular, have been subject to numerous investigations, and precise thermochemical data are now available. Weisshaar and co-workers have used resonance-enhanced multiphoton ionization (REMPI) and ZEKE spectroscopy to obtain an accurate ionization potential for benzyl radical (7.2477 ± 0.0017 and 7.2488 ± 0.0006 eV, respectively).[7,8] Ellison and co-workers found the C−H bond energy of the methyl group in toluene to be 89.8 ± 0.5 kcal/mol[9] using the measured gas-phase acidity of toluene together with the electron affinity of benzyl radical, which, in turn, had been determined previously using negative ion photoelectron spectroscopy.[10] From the photoelectron spectrum of the benzyl anion, Gunion et al.[10] obtained an electron affinity of 0.912 ± 0.006 eV and identified two active vibrational modes. We have now extended these studies to examine the effects of halogen substitution on the properties of benzyl radical. We have measured photoelectron spectra of the ortho, meta, and para halosubstituted benzyl anions (**1**, **2**, and **3**, respectively), where the halogen substituents include fluorine, chlorine, and bromine (**a**, **b**, and **c**, respectively), for a total of nine different species.

Previous spectroscopic studies of the halobenzyl radicals have primarily involved the use of emission and fluorescence techniques. Carlton and Thrush studied the visible LIF spectra of the fluorobenzyl radicals **1a**, **2a**, and **3a**.[11] Fukushima and co-workers studied the *p*-fluorobenzyl radical[2,12] and the *p*-chlorobenzyl radical[5,13] using laser-induced fluorescence.

Examination of substituent effects using negative ion photoelectron spectroscopy serves two purposes. First, it is possible to determine the extent to which substitution affects the thermochemical properties. By examination of the effects of substituents in different ring positions, it is possible to identify the physical origins of the effects. Second, substitution of the benzylic system provides additional help in identifying the active vibrational modes in the photoelectron spectrum. For instance, substitution in the para position maintains the symmetry of the benzyl radical and does not introduce additional active modes into the spectrum. However, it can change some vibrational frequencies. In contrast, substitution in the ortho or meta positions reduces the symmetry to C_s and additional vibrational modes will be present in the photoelectron spectrum. Moreover, the differences between the spectra for the different halogen substituents provide assistance in assigning the observed vibrational frequencies.

In this paper, we report the electron affinities of the halobenzyl radicals, as determined from photoelectron spectroscopy of the corresponding halosubstituted benzyl anions. We show that halogen substitution has an effect on the electron affinity of the benzyl radical that is highly dependent on the position of the substituent (ortho, meta, or para) and on the identity of the halogen. Overall, the substituent effects on the electron affinities of halobenzyl radicals reflect the substituent effects on the gas-phase acidities of the halobenzyl toluenes. From our measured EAs and the gas-phase acidities of the halotoluenes, we calculate the benzylic C−H bond energies. We find that the C−H bond energies of the halotoluenes are similar to each other and, moreover, are similar to the C−H bond energy in the hydrocarbon. Finally, several vibrational frequencies are reported for each of the species addressed here,

† Present address: Spectralogic Corp., Boulder, CO.
‡ Present address: Department of Chemistry, Purdue University, West Lafayette, IN.

10834 *J. Phys. Chem. A, Vol. 103, No. 50, 1999*

Kim et al.

and the vibrational modes are assigned with the assistance of electronic structure calculations.

Experimental Section

The experiments were carried out using the negative ion photoelectron spectrometer that has been described in detail elsewhere;[14,15] here, we provide only a brief description with an emphasis on specific halobenzyl ion production. The apparatus consists of three major components: an ion source, a mass filter, and a laser photodetachment and electron energy analysis region.

Halobenzyl ions are produced in a liquid nitrogen cooled flowing afterglow ion source. First, O^- ions are formed in a microwave discharge cavity with a small amount of O_2 seeded in ca. 0.5 Torr of helium buffer gas. The O^- ions are then carried through the flow tube by the helium buffer gas and allowed to react with neutral reagents that are introduced through ring inlets at various points along the flow tube. Addition of methane through a ring inlet situated just beyond the microwave discharge source produces OH^-. The halobenzyl ions are prepared by proton transfer between the OH^- and *o*-, *m*-, or *p*-halotoluene added through a second ring inlet situated further downstream. Although hydroxide is capable of deprotonating ring positions in haloaromatic molecules,[16] it is energetically most favorable to deprotonate at the methyl group.[17] Typical halobenzyl ion currents of 30−100 pA could be prepared in this fashion.

Halobenzyl ions prepared in the flowing afterglow are thermalized by collisions to the temperature of the surrounding helium buffer gas. Ion cooling is achieved by passing liquid nitrogen through a metal jacket surrounding the flowing afterglow. The halobenzyl ions formed under these conditions have temperatures estimated to be ca. 175 K based on intensities of hot bands in the photoelectron spectra.[18]

After production, ions are gently extracted from the flowing afterglow source through a 1 mm aperture into a differentially pumped region. Within this region, they are accelerated to 735 eV, focused, and mass-selected using a Wien velocity filter ($M/\Delta M \approx 40$). The mass-selected halobenzyl ions are then decelerated to 40 eV and injected into the laser interaction region where they intersect the output of an argon ion laser (351 nm), amplified to ∼100 W by an external power buildup cavity.[19] A small solid angle of the photodetached electrons is subsequently collected and energy-analyzed by a hemispherical analyzer and detected using a position-sensitive microchannel plate detector, with an overall resolution of ∼8 meV.

The resulting photoelectron spectra depict the number of photoelectrons, integrated over many scans, versus the electron binding energy (eBE), the difference between the photon energy (3.53119 eV) and the electron kinetic energy (eKE). The measured electron energies are converted to an absolute center-of-mass eKE by scaling relative to the $^3P_2 + e^- \leftarrow {}^3P_{3/2}$ peak in the photoelectron spectrum of O^- [EA(O) = 1.46112 eV].[20] A small (∼1%) compression factor of the electron kinetic energy scale, γ, is determined by comparing the measured positions of the fine-structure peaks of W^- with the known term energies of tungsten atom.[21]

Materials. All reagents were obtained from commercial suppliers and used as received. The halotoluenes were obtained from Sigma-Aldrich: *o*-fluorotoluene (99+%), *m*-fluorotoluene (99%), *p*-fluorotoluene (97%), *o*-chlorotoluene (99%), *m*-chlorotoluene (98%), *p*-chlorotoluene (98%), *o*-bromotoluene (98%), *m*-bromotoluene (98%), and *p*-bromotoluene (98%). Gas purities were 99.995% for He and 99% for O_2.
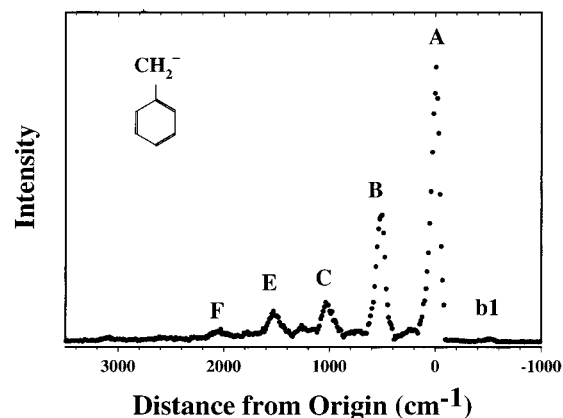
Figure 1. The 351 nm photoelectron spectrum of benzyl anion plotted as electron counts vs electron binding energy with zero eBE set at the adiabatic EA.

Results

The 351 nm photoelectron spectra for the halobenzyl anions examined in this work are shown in Figures 1−4. For the ortho-, meta-, and para-substituted benzyl anion spectra (Figures 2−4, respectively), a spectrum of the unsubstituted benzyl anion is also shown for comparison. The intense peaks labeled A in the spectra correspond to the origins of the spectral bands. The energies of these peaks are the electron affinities of the corresponding benzyl radicals and are listed to the right of each spectrum. In addition, vibrational peaks are also observed for each species. To simplify comparisons between systems, we present the spectra on relative energy scales. In the following sections, we describe the features of each spectrum in more detail, beginning with the benzyl anion.

Benzyl. The photoelectron spectrum of the benzyl anion, created in a liquid nitrogen cooled flowing afterglow source, is shown in Figure 1. The spectrum closely resembles that reported previously by Gunion et al.,[10] obtained without cooling. The adiabatic electron affinity of benzyl radical is 0.912 ± 0.006 eV, and two vibrational progressions are observed in the spectrum. The peak spacing in one vibrational progression (peaks B and C) is 515 ± 15 cm^{-1}. The second progression begins at peak E, and the spacing between the origin and the beginning of this progression is 1510 ± 25 cm^{-1}. Peak F is a combination band with one quantum in each of the two fundamental vibrations. Finally, b1 is a hot band, yielding an anion vibrational frequency of 514 ± 15 cm^{-1}. These results agree with those reported previously.[10] The Franck−Condon factors for the photodetachment of the benzyl anion can be determined using a modeling procedure that has been described previously. The relative intensities of the vibrational transitions depend on the geometry difference between the anion and neutral along its vibrational coordinate.[22,23] The Franck−Condon factors obtained by fitting the spectra are the "normal coordinate displacements", ΔQ_i, the elements of the Duschinsky **K** matrix.[24] The normal coordinate displacements obtained for the vibration frequencies listed above using the fitting procedure described elsewhere[14] are listed in Table 1. The larger displacement is found for the lower frequency mode, indicating the greatest geometry change between the anion and the neutral along that coordinate.

The two active vibrational modes observed in the spectrum of benzyl are also found in the spectra of the halobenzyl anions. However, in those systems additional modes are also found to be active, depending on the symmetry of the molecule. In the

o-, *m-*, and *p-*Halobenzyl Anions

J. Phys. Chem. A, Vol. 103, No. 50, 1999 **10835**

TABLE 1: Experimentally Determined Values from This Work

R	EA (eV)	observed radical vibrations[a] (cm^{-1})	observed ion vibrations[b] (cm^{-1})	ΔQ_i (amu$^{1/2}$ Å)	DH$_{298}$(R−H) (kcal mol^{-1})
benzyl[c]	0.912 ± 0.006	514 ± 15	514 ± 15	0.28	89.8 ± 0.5
		1510 ± 25		0.08	
ortho					
fluoro, **1a**	1.091 ± 0.008	440 ± 20	425 ± 40	0.200	-
		550 ± 20		0.185	
		770 ± 40		0.090	
		1290 ± 40		0.060	
		1550 ± 40		0.085	
chloro, **1b**	1.257 ± 0.008	560 ± 20		0.235	89.0 ± 3.1
		1250 ± 40		0.052	
		1540 ± 40		0.080	
bromo, **1c**	1.308 ± 0.008	550 ± 20		0.258	90.2 ± 3.1
		1230 ± 40	530 ± 30	0.063	
		1540 ± 40		0.082	
meta					
fluoro, **2a**	1.173 ± 0.008	520 ± 20	510 ± 20	0.245	88.8 ± 2.1
		750 ± 40		0.031	
		1540 ± 40		0.092	
chloro, **2b**	1.272 ± 0.008	525 ± 20	490 ± 20	0.265	89.8 ± 2.1
		670 ± 40		0.032	
		1520 ± 40		0.095	
bromo, **2c**	1.307 ± 0.008	525 ± 20	500 ± 20	0.240	90.1 ± 3.1
		1520 ± 40		0.100	
para					
fluoro, **3a**	0.937 ± 0.008	445 ± 20	420 ± 20	0.388	87.6 ± 2.1
		1500 ± 40		0.095	
chloro, **3b**	1.174 ± 0.008	375 ± 20	365 ± 20	0.387	87.5 ± 2.1
		1520 ± 40		0.074	
bromo, **3c**	1.229 ± 0.008	290 ± 20	265 ± 40	0.435	88.5 ± 3.1
		1510 ± 40		0.075	

[a] Determined from average peak spacings. See Tables 2−4. [b] Determined from peak positions of hot bands. See Tables 2−4. [c] From ref 10.

following three sections, we address the spectra observed in the case of ortho, meta, and para substitution, respectively.

_o_-Halobenzyl. The photoelectron spectra of the *o*-fluorobenzyl, chlorobenzyl, and bromobenzyl anions **1a**⁻, **1b**⁻, and **1c**⁻, respectively, are shown in Figure 2, and the experimentally determined parameters are summarized in Table 1. The energies of the origin peaks in the spectra give adiabatic electron affinities (EA) for the radicals: EA(**1a**) = 1.091 ± 0.008 eV, EA(**1b**) = 1.257 ± 0.008 eV, and EA(**1c**) = 1.308 ± 0.008 eV. Two vibrations are observed in all the ortho spectra and have frequencies similar to those in the benzyl spectrum. As in benzyl, peaks B and C correspond to the lower frequency mode (although peak C is slightly obscured in the **1a**⁻ spectrum). The frequency of this mode is found to be ca. 550 cm^{-1}, slightly higher than that in benzyl. The peaks labeled E in the *o*-halobenzyl anion spectra are found near 1550 cm^{-1}, essentially unchanged from that in unsubstituted benzyl. Three additional radical vibrations are observed in the ortho spectra that correspond to neither combination bands nor overtone transitions of those listed above and are therefore assigned as fundamentals of additional normal modes. All the ortho spectra contain peaks (labeled D) at ~1200 cm^{-1}. This mode appears lower in frequency for larger halogen substituents. On the other hand, there are two additional modes that appear to be only active in the spectrum of **1a**⁻. Peak a is the second most intense vibration seen in the spectrum of **1a**⁻ but is not observed in the spectra of the other ortho systems. The peak spacing between A and a indicates a vibrational frequency of 440 ± 20 cm^{-1}. Given this assignment, peak c in the **1a**⁻ spectrum is readily identified as a combination of the modes at 550 and 440 cm^{-1}. Another vibration that is unique to the spectrum of **1a**⁻ is labeled b and corresponds to a vibrational frequency of 770 ± 20 cm^{-1}.

Weak hot bands are observed in the spectra of **1a**⁻ and **1c**⁻. The hot band in the spectrum of **1c**⁻ is displaced by 530 cm^{-1}, comparable to that observed in the benzyl spectrum. This peak is labeled a1. The hot band observed in the spectrum of **1a**⁻ indicates an ion frequency of 425 cm^{-1}, different from that observed for benzyl or **1c**⁻. Therefore, the hot band likely corresponds to a different mode in **1a**⁻, and we label the peak b1. The positions of all the identified peaks for the ortho isomers are listed in Table 2. The Franck−Condon factors for the transitions were obtained by modeling the spectra. The Franck−Condon factors for each mode obtained from the fits are summarized in Table 1.

_m_-Halobenzyl. The photoelectron spectra of the *m*-fluorobenzyl, *m*-chlorobenzyl, and *m*-bromobenzyl ions are shown in Figure 3. The positions of the origins (labeled A) indicate electron affinities of 1.173 ± 0.008, 1.272 ± 0.008, and 1.307 ± 0.008 eV for, **2a**, **2b**, and **2c**, respectively. For the meta isomers, two neutral vibrations are clearly active in all three spectra, with the $v = 1$ peaks labeled as B and E once again. The frequencies for these modes are listed in Table 1. Overtone (C) and combination peaks (F, G, and H) are also observed. The magnitudes of the vibrational frequencies and their associated Franck−Condon factors are comparable to those for identically labeled peaks in the benzyl spectrum (Table 1). In addition, all three spectra for the meta-substituted ions contain hot band peaks (labeled a1), yielding vibrational frequencies for the corresponding anions.

In addition to those vibrations listed above that are common to all three systems, we also observe another active mode (peak a) in the *m*-fluorobenzyl and *m*-chlorobenzyl spectra, with vibrational frequencies of 750 and 670 cm^{-1}, respectively. The peak corresponding to this mode in the **2c**⁻ spectrum is likely obscured by peak B. The positions of all the observed peaks in the spectra of the meta isomers are listed in Table 3.

_p_-Halobenzyl. The photoelectron spectra of the *p*-fluorobenzyl, *p*-chlorobenzyl, and *p*-bromobenzyl anions (**3a**⁻, **3b**⁻, and
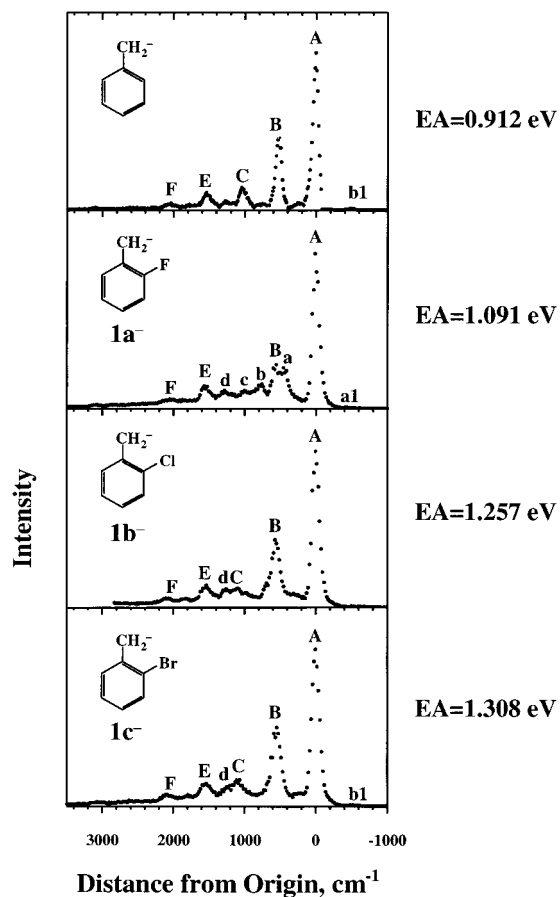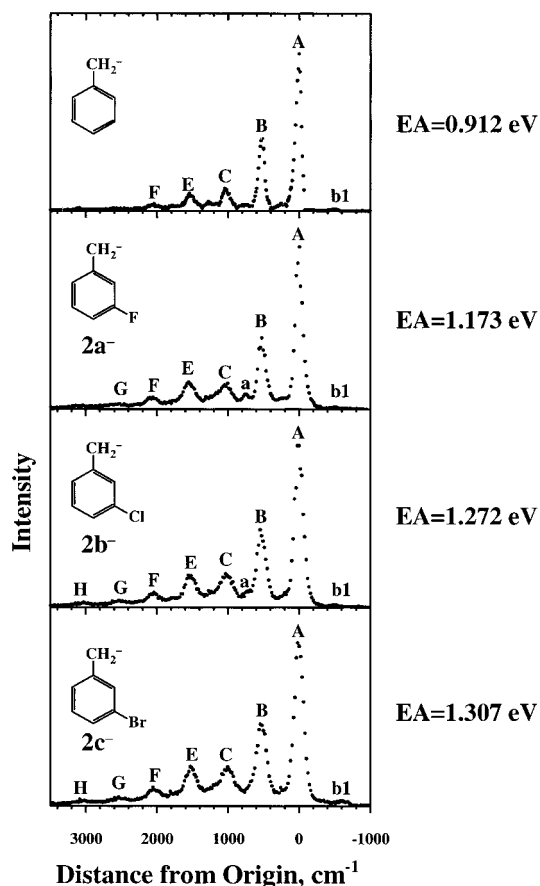
Figure 2. The 351 nm photoelectron spectra of the *o*-halobenzyl anions. Each data set is plotted as electron counts vs electron binding energy with zero eBE set at the adiabatic EA for that species. The binding energy at the origin (EA) is given to the right of each spectrum. Assignments of the labeled peaks are provided in Table 2.

TABLE 2: Peak Positions[a] and Assignments for the Spectra of *o*-Halobenzyl Anions

peak[b]	assignment[c]	fluoro	chloro	bromo
a1	23_1^0	−425		
b1	22_1^0			−530
A	0_0^0	0	0	0
a	23_0^1	440		
B	22_0^1	550	560	550
b	21_0^1	770		
c	$22_0^1 23_0^1$	990		
C	22_0^2		1110	1100
D	13_0^1	1290	1250	1230
E	7_0^1	1550	1540	1540
F	$7_0^1 22_0^1$	2060	2090	2080

[a] Peak positions relative to the origin peak. [b] Peaks labeled in Figure 2. [c] See normal modes illustrated in Figures 5 and 6.

3c⁻, respectively) are shown in Figure 4. The measured spectra of the *p*-fluorobenzyl and *p*-bromobenzyl anions contain small contributions from the corresponding meta isomers, as indicated by the presence of peaks at 1.173 and 1.307 eV, respectively, the origins of the meta photoelectron bands. Therefore, scaled meta spectra have been subtracted from the measured spectra of **3a⁻** and **3c⁻** to give the ortho and para spectra shown in Figure 4. The band origins (A) of the photoelectron spectra yield electron affinities of 0.937 ± 0.008 eV, 1.174 ± 0.008 eV, and 1.229 ± 0.008 eV for **3a**, **3b**, and **3c**, respectively. Again, each spectrum contains a dominant vibrational progression (peaks B, C, and D) and a weaker vibrational progression (E, F, and

Figure 3. The 351 nm photoelectron spectra of the *m*-halobenzyl anions. Each data set is plotted as electron counts vs electron binding energy with zero eBE set at the adiabatic EA for that species. The binding energy at the origin (EA) is given to the right of each spectrum. Assignments of the labeled peaks are provided in Table 3.
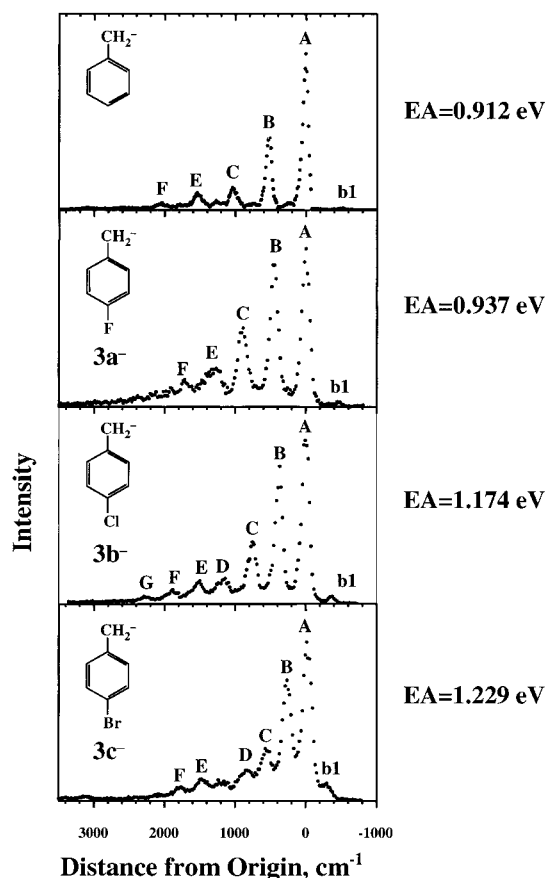
TABLE 3: Peak Positions[a] and Assignments for the Spectra of *m*-Halobenzyl Anions

peak[b]	assignment[c]	fluoro	chloro	bromo
b1	22_1^0	−510	−490	−500
A	0_0^0	0	0	0
B	22_0^1	520	525	525
a	21_0^1	750	670	
C	22_0^2	1030	1030	1010
E	7_0^1	1540	1520	1520
F	$7_0^1 22_0^1$	2060	2040	2040
G	$7_0^1 22_0^2$	2570	2520	2510
H	$7_0^1 22_0^3$		3030	3020

[a] Peak positions relative to the origin peak. [b] Peaks labeled in Figure 3. [c] See normal modes illustrated in Figures 5 and 6.

G) at higher frequency (Table 1). Unlike what is found for the ortho and meta isomers, the vibrational frequency of the mode near 500 cm⁻¹ is found to be dependent on the halogen substituent. Vibrational frequencies of 445, 375, and 285 cm⁻¹ are found for the fluoro-, chloro-, and bromo-substituted ions, respectively, which are lower than the values of 500−550 cm⁻¹ observed for the other systems.

As was found in the other systems, the higher frequency progression begins with peak E, and the frequency of the active mode is not dependent on the halogen. In the spectrum of **3a⁻**, peak E partially overlaps with peak D, which makes it difficult to measure its energy. However, the frequency of the mode can be determined more reliably using peak F, the combination band. Last, weak hot bands are observed in all spectra and are labeled

o-, *m*-, and *p*-Halobenzyl Anions

J. Phys. Chem. A, Vol. 103, No. 50, 1999 **10837**

Figure 4. The 351 nm photoelectron spectra of the *p*-halobenzyl anions. Each data set is plotted as electron counts vs electron binding energy with zero eBE set at the adiabatic EA for that species. The binding energy at the origin (EA) is given to the right of each spectrum. Assignments of the labeled peaks are provided in Table 4.

TABLE 4: Peak Positions^a and Assignments for the Spectra of *p*-Halobenzyl Anions

peak^b	assignment^c	fluoro	chloro	bromo
b1	13^0_1	-420	-365	-265
A	0^0_0	0	0	0
B	13^1_0	445	375	285
C	13^2_0	890	750	580
D	13^3_0	1340	1150	870
E	4^1_0	1500	1520	1510
F	$4^1_0 13^1_0$	1950	1880	1760
G	$4^1_0 13^2_0$		2260	

^{a} Peak positions relative to the origin peak. ^{b} Peaks labeled in Figure 4. ^{c} See normal modes illustrated in Figure 5.

a1. The ion frequencies obtained from the hot bands are 420, 365, and 265 cm^{-1} for **3a$^-$**, **3b$^-$**, and **3c$^-$**, respectively. The positions of all the peaks are listed in Table 4.

Comparison of the spectra shown in Figure 4 with the spectrum of benzyl shows that substitution in the para position has only a small effect on the intensities of the vibrational peaks. This aspect is reflected by the Franck−Condon factors for these systems, which are comparable to those for benzyl (Table 1).

Angular Distributions. The angular dependence of the photoelectron signal is given by

$$I(\theta) = \frac{\sigma_{tot}}{4\pi}\left[1 + \frac{\beta(3\cos^2\theta - 1)}{2}\right] \qquad (1)$$

where θ is the angle between the electric field vector of the

laser and the electron collection direction, σ_{tot} is the total photodetachment cross section, and β is the anisotropy parameter $(-1 \leq \beta \leq 2)$.[25−28] The photoelectron spectra for the halobenzyl anions shown in Figures 1−4 were obtained with $\beta = 54.7°$ ("magic angle"), at which the signal is independent of the anisotropy parameter. The photoelectron spectra were also measured with two other laser polarizations, $\theta = 0°$ and 90°. From the photodetachment yields at these two angles, I_0 and I_{90}, respectively, the anisotropy parameter can be calculated via the relationship shown in

$$\beta = \frac{I_0 - I_{90}}{0.5I_0 + I_{90}} \qquad (2)$$

The anisotropy parameter, β, depends on both the nature of the orbital from which the electron is detached and the kinetic energy of the detached electron. For atomic ions, detachment from an s orbital results in formation of a p wave ($l = 1$) continuum electron, with $\beta = +2$, independent of electron kinetic energy. In contrast, detachment of an electron from a p orbital results in formation of both s and d wave ($l = 0$ and 2, respectively) continuum electrons, making β energy-dependent. For photon energies near the threshold for electron detachment from a p orbital, the s wave component of the continuum electron dominates and $\beta = 0$, while at photon energies ~1 eV above threshold, the d wave component becomes more important and $\beta = -1$.[28] In contrast to atomic anions, electron detachment from molecular anions is less straightforward. For the electron kinetic energy range in these studies, it has been found[29,30] that, in general, β is positive for detachment from σ (s-like) orbitals, and negative for detachment from π (p-like) orbitals. Therefore, the photoelectron angular distribution provides a signature for the orbital from which the electron was detached.

The anisotropy parameters obtained for detachment of the halobenzyl anions range from -0.21 to -0.68. These values are all similar to those previously reported[10,18,31,32] for photodetachment of π electrons with electron kinetic energies in the same range.

Molecular Orbital Calculations. Molecular orbital calculations have been carried out on the radicals examined in this study in order to assist the vibrational assignments. Frequencies were calculated for the optimized geometries at the Becke3LYP/6-31+G* level of theory using the Gaussian 94 program.[33] The frequencies for the totally symmetric modes, those that can be active in the photoelectron spectra, are listed in Table 5. Calculations at the B3LYP/6-31+G* level of theory have also been carried out on the ions. A complete listing of all the frequencies and the optimized geometries for the ions and the radicals are provided in Supporting Information.

Discussion

In this section, we examine the results of the photoelectron measurements. In the first part, the thermochemical properties of the halotoluene species are discussed. The measured electron affinities are used along with the gas-phase acidities to derive homolytic bond energies. In addition, we present a simple model based on π-donor and σ-withdrawing effects to account for the trends in the electron affinities. In the last section, we discuss the vibrational structure observed in the spectra and propose vibrational assignments.

Thermochemistry. The measured electron affinities for halobenzyl radicals can be used to derive the dissociation enthalpies (DH$_{298}$(R−H)) of the C−H bond in the methyl group of a given halotoluene. The bond enthalpy is related[34] to the

TABLE 5: Vibrational Frequencies for Totally Symmetric Modes Calculated at the B3LYP/6-31+G* Level of Theory[a]

	ortho, C_s			meta, C_s			para, C_{2v}		
	fluoro	chloro	bromo	fluoro	chloro	bromo	fluoro	chloro	bromo
ν_1	3284	3287	3287	3266	3266	3266	3217	3217	3218
ν_2	3220	3218	3220	3227	3226	3227	3192	3189	3189
ν_3	3208	3207	3208	3213	3210	3213	3171	3171	3171
ν_4	3198	3196	3197	3204	3202	3202	1613	1595	1593
ν_5	3186	3188	3188	3188	3186	3186	1523	1519	1520
ν_6	3183	3182	3182	3173	3173	3173	1512	1507	1507
ν_7	1613	1601	1599	1612	1593	1591	1295	1298	1301
ν_8	1583	1572	1570	1593	1573	1571	1251	1196	1198
ν_9	1512	1513	1512	1515	1515	1514	1170	1096	1082
ν_{10}	1501	1479	1479	1498	1498	1498	1017	1010	1006
ν_{11}	1477	1463	1461	1462	1445	1444	850	834	833
ν_{12}	1351	1338	1337	1357	1348	1351	759	646	608
ν_{13}	1306	1297	1295	1325	1327	1330	459	380	295
ν_{14}	1292	1291	1297	1289	1271	1273			
ν_{15}	1218	1186	1188	1200	1190	1193			
ν_{16}	1180	1159	1157	1170	1131	1136			
ν_{17}	1142	1063	1063	1111	1094	1086			
ν_{18}	1051	1046	1031	1017	993	991			
ν_{19}	976	978	979	995	991	987			
ν_{20}	866	848	847	947	894	876			
ν_{21}	767	682	666	751	692	672			
ν_{22}	583	564	558	538	534	535			
ν_{23}	520	448	432	513	412	390			
ν_{24}	433	374	301	447	395	308			
ν_{25}	302	270	228	305	241	201			

[a] Values in cm^{-1}.

TABLE 6: Thermochemical Properties of Halobenzyl Radicals and Halotoluenes

halobenzyl (R)	EA(R) (kcal/mol)	ΔH_{acid}(R−H)[a] (kcal/mol)	DH$_{298}$(R−H)[b] (kcal/mol)
benzyl	21.03 ± 0.14	382.3 ± 0.5	89.8 ± 0.6
ortho			
fluoro	25.16 ± 0.18		
chloro	28.99 ± 0.18	373.6 ± 3.1	89.0 ± 3.1
bromo	30.16 ± 0.18	373.6 ± 3.1	90.2 ± 3.1
meta			
fluoro	27.05 ± 0.18	375.4 ± 2.1	88.8 ± 2.1
chloro	29.33 ± 0.18	374.1 ± 2.1	89.8 ± 2.1
bromo	30.14 ± 0.18	373.6 ± 3.1	90.1 ± 3.1
para			
fluoro	21.61 ± 0.18	379.6 ± 2.1	87.6 ± 2.1
chloro	27.07 ± 0.18	374.0 ± 2.1	87.5 ± 2.1
bromo	28.34 ± 0.18	373.7 ± 3.1	88.5 ± 3.1

[a] Values from ref 17 unless otherwise noted. [b] Calculated using eq 3.

electron affinity according to

$$DH_{298}(R-H) = EA(R) + \Delta H_{acid}(R-H) - IP(H) \quad (3)$$

where ΔH_{acid}(R−H) refers to the 298 K gas-phase acidity of a halotoluene, EA(R) is the electron affinity of the radical, and IP(H) is the ionization energy of atomic hydrogen (313.59 kcal/mol). The small (<0.3 kcal/mol) temperature correction term[34] is ignored. The gas-phase acidities of the *o*-, *m*-, and *p*-halotoluenes have been reported previously[17,35] and are listed in Table 6. The 298 K bond dissociation enthalpies obtained using the gas-phase acidities and the electron affinities measured in this work are also included in Table 6. The bond energies for the halotoluenes measured in this study are all within error of each other and are about 89 kcal/mol. Moreover, they also agree, within error, to the C−H bond energy in unsubstituted toluene, 89.8 ± 0.6 kcal/mol.[9] Therefore, halogen substitution does not affect the strength of the C−H bond in toluene.

Substituent Effects on the Electron Affinity. The electron affinities for the isomeric halobenzyl radicals follow a distinct

TABLE 7: Electron Affinities of Halobenzyl Radicals Calculated at the B3LYP/6-31+G* Level of Theory[a]

	ortho	meta	para
fluoro	1.120 (1.173)	1.040 (1.091)	0.901 (0.937)
chloro	1.182 (1.257)	1.201 (1.272)	1.107 (1.174)
bromo	1.150 (1.229)	1.230 (1.308)	1.228 (1.307)

[a] Values are in eV and include correction for zero-point vibrational energy differences. Values in parentheses are experimentally determined electron affinities.

pattern. For each substituent, the meta isomer has the highest electron affinity, while the ortho and para isomers have consecutively lower EAs. Moreover, for a given isomer, the bromo derivative has the highest electron affinity, while the electron affinities of the chloro- and fluoro-substituted species are sequentially lower. The electron affinity of the bromo-derivative is also less dependent on the position of the halogen. These trends are consistent with what is expected given the electronic structure of the benzyl system and the known inductive and resonance properties of the halogen substituents.[36] Substitution in the ortho and para positions should destabilize the ion because of π donation, leading to lower electron affinities for these isomers. However, a halogen substituent in the ortho position is more favorable than one in the para position because of inductive effects, and the ortho substituent is closer to the highest charge density site. Last, the larger, more polarizable substituents are better at stabilizing the negative ion and lead to higher electron affinities.

The trends observed in the electron affinities of the halobenzyl radicals are reproduced very well at the B3LYP/6-31+G* level of theory. The calculated electron affinities are listed in Table 7. For these systems, the calculated electron affinities are systematically low, by ca. 35−50 meV for the fluorinated radicals and 70−80 meV for the other halogenated systems. It should be emphasized that even considering the systematic error, the agreement between the calculated and experimental electron affinities is excellent. This is consistent with other recent observations that density functional theory provides accurate electron affinities at a modest computational cost.[37−39]

At a more qualitative level, the trends observed in the electron affinities of the halobenzyl radicals mirror those found for the halotoluene acidities.[36] This is to be expected, however, because the C−H bond dissociation energies are essentially the same for all species involved. In that case, eq 3 reduces to EA(R) = $M - \Delta H_{acid}$(R−H), where $M = $ DH$_{298}$(R−H) + IP(H) = 403 kcal/mol.

Vibrational Assignments. In this section, we discuss the assignments of the vibrational frequencies. Much of the analysis relies on the results reported previously for benzyl, and therefore, we begin by examining that system.

Benzyl. Two modes of benzyl radical are active in the photoelectron spectrum, with frequencies of 514 and 1510 cm^{-1}. The mode with the 514 cm^{-1} frequency is readily assigned to ring deformation, which Gunion et al.[10] labeled as ν_{13}, similar to the ν_{6a} mode in benzene.[40] This type of vibrational mode is observed for most aromatic ring species that have been examined using photoelectron spectroscopy, including phenyl,[10] phenoxyl,[10] and even *m*-xylylene[41] and *o*- and *p*-benzyne.[42,43]

The higher frequency vibration is more difficult to assign. Experimental[44] and computational[10] studies indicate that there are three a$_1$ vibrational modes near 1500 cm^{-1}. Gunion et al.[10]
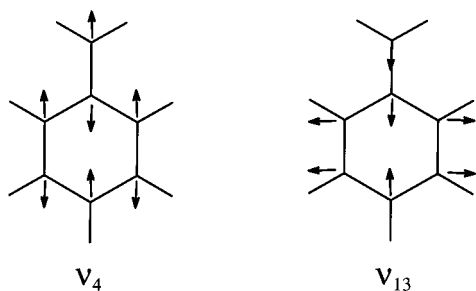
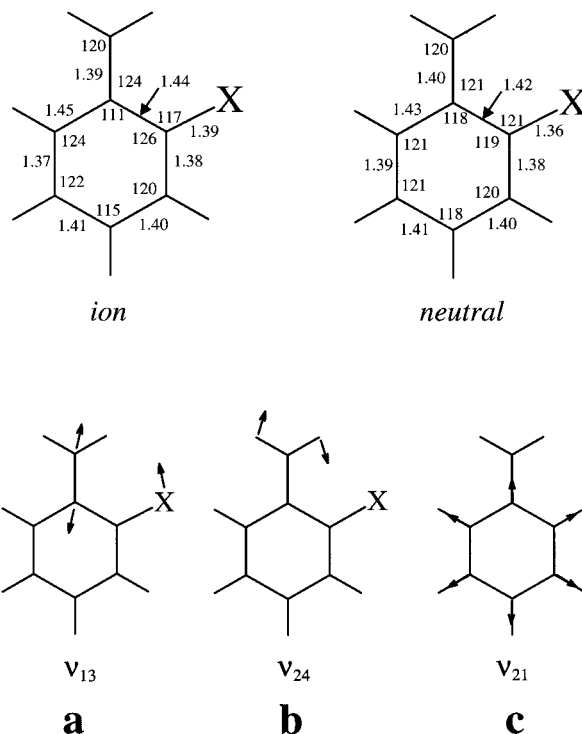**Figure 5.** Calculated normal modes for vibrations observed in the benzyl spectra.

Figure 6. Calculated geometries of *o*-fluorobenzyl anion and radical and calculated normal mode vibrations observed in the *o*-fluorobenzyl spectra (a−c). For the C_s isomers, the vibrational modes labeled as ν_4 and ν_{13} in Figure 5 correspond to ν_7 and ν_{22}, respectively.

assigned this frequency to a mode containing significant C−CH$_2$ stretching, which is overall best described as a ring stretching mode, ν_4. This assignment was made on the basis of comparison between experimental and calculated frequencies, as well as the spectrum of phenoxide, in which a similar vibrational frequency is obtained. Given the similarity between the systems, it is argued that the active modes are the same. This appears to rule out the possibility that the 1510 cm^{-1} frequency is for a mode involving significant H−C−H bending, ν_5. The normal coordinates corresponding to the assigned frequencies are shown in Figure 5.

Para. The spectra obtained for the para isomers are the simplest for the substituted species, with only two active vibrational modes. Because the para isomers have the same symmetry as benzyl, the two active modes would be expected to be the same as those described in the previous section. For example, the lower frequency mode is likely the ring deformation, and the measured frequencies are 445, 375, and 285 cm^{-1} for **3a**, **3b**, and **3c**, respectively. These are in reasonable agreement with the frequencies calculated for ν_{13} listed in Table 5. More importantly, the halogen dependence predicted by theory for this frequency is consistent with the experimental results. The vibrational frequencies for the ion obtained from the hot bands in the spectra are assigned to similar vibrational modes.

By comparison with benzyl, it is expected that the observed frequency around 1500 cm^{-1} should correspond to a mode with significant C−CH$_2$ stretching character. The calculated mode that is analogous to that in benzyl is ν_4, at 1590−1610 cm^{-1}. The calculated frequencies are in reasonable agreement with the measured values, especially after accounting for anharmonicity in the vibrational potential and, moreover, do not a predict a strong halogen dependence. Therefore, the results for the para-substituted systems support the assignment of the 1500 cm^{-1} frequency to the ring stretching mode.

The calculated frequencies for ν_5, ~1520 cm^{-1}, are also in reasonable agreement with the measured frequencies and also do not exhibit a strong dependence on the halogen substitute. The vibrational mode for ν_5 is essentially H−C−H bending at the α position. However, although ν_5 is possibly the observed frequency, it is considered unlikely because (1) calculated frequencies are more likely to overestimate the frequency because of anharmonic effects and (2) the comparison with the phenoxyl system suggests that the high-frequency mode does not contain significant amounts of H−C−H bending. Therefore, the ~1500 cm^{-1} frequencies for **3a**−**3c** more likely correspond to the ring stretching modes.

Ortho. Because of the lower symmetry, the spectra of the *o*-halobenzyl anions are more complicated than those of benzyl or the para isomers. Three vibrational modes are clearly observed in all three systems, and two additional vibrations are observed in the *o*-fluorobenzyl spectrum.

As in the spectra of benzyl and *p*-halobenzyl anions, the main progression in the *o*-halobenzyl spectra is assigned to the ring deformation mode. Vibrational frequencies are found for this mode at 550 ± 20, 560 ± 20, and 550 ± 20 cm^{-1} for **1a**, **1b**, and **1c**, respectively. The fact that they are insensitive to the actual halogen substituent while those for **3a**−**3c** are halogen-dependent indicates that the ortho site is not as involved in the vibrational motion as the para site. The hot band in the *o*-bromobenzyl anion spectrum is assigned to the same mode. The calculated frequencies for ν_{22} are 583, 564, and 558 cm^{-1}, respectively (see Table 5), which are only about 3% higher than the experimental results.

The spectra for the ortho isomers also exhibit a weaker vibration near 1500 cm^{-1}. Again, this is assigned to the ring stretching mode, which is ν_7. The calculated frequencies for this mode are 1613, 1601, and 1599 cm^{-1} for **1a**, **1b**, and **1c**, respectively, and are only slightly higher than our measured values of 1550 ± 40, 1540 ± 40, and 1540 ± 40 cm^{-1}, respectively. As in the case of the para isomer, it is possible that this mode is the H−C−H bending mode, ν_9, with calculated frequencies of 1512, 1513, and 1512 cm^{-1} for **1a**, **1b**, and **1c**, respectively. However, as with para, this assignment is considered unlikely.

A third vibrational frequency is observed for all three ortho isomers, with values of 1290 ± 40, 1250 ± 40, and 1230 ± 40 cm^{-1} for the *o*-fluorobenzyl, chlorobenzyl, and bromobenzyl radicals, respectively. In this case, the frequencies obtained from the molecular orbital calculations are of limited assistance because there are three vibrational modes predicted to have frequencies in this region. However, the calculated geometries provide additional insight. The geometries of the *o*-fluorobenzyl anion and radical, calculated at the B3LYP level of theory, are shown in Figure 6. Among the largest differences between the geometry of the ion and the radical is in the C$_{ipso}$−C$_{ortho}$−F bond angle, which is 4° larger in the neutral. This is significant

because the calculated frequency near 1300 cm^{-1} (ν_{13}) corresponds to bending of that angle (Figure 6a). Moreover, because this bending motion is only totally symmetric under C_s symmetry, this mode should not be active in the spectra of the benzyl anion or the para-substituted species. The calculated spectra of the *o*-halobenzyl anions, obtained using geometries and frequencies from the molecular orbital calculations according to a procedure described elsewhere,[45] agree well with the measured spectra, supporting our assignments.

The remaining vibrational modes for the ortho species are only observed for the *o*-fluoro isomer. An intense peak is found at 440 $\pm$ 20 cm^{-1}. On the basis of the molecular orbital calculations, this frequency most likely corresponds to the CH$_2$ rocking mode, ν_{24}, of the radical. The calculated frequency is 433 cm^{-1}, and the motion is illustrated in Figure 6b. In addition, a hot band peak is observed at 425 $\pm$ 40 cm^{-1} for this mode in the spectrum of **1a**$^-$. Given its intensity in the spectrum of **1a**$^-$, it is surprising that the mode is too weak to be observed in the *o*-chloro and bromobenzyl spectra.

The transition at 770 $\pm$ 40 cm^{-1} also appears exclusively in the spectrum of **1a**$^-$. This is possibly a ring breathing mode, ν_{21}, illustrated in Figure 6c, with a calculated frequency of 767 cm^{-1}. In addition, the calculations predict that substitution by heavier halogens should shift the frequency significantly to 682 and 666 cm^{-1} for the chloro and bromo systems, respectively. Weak transitions at those frequencies would not be well resolved from the intense peaks near 550 cm^{-1} (peak B).

Meta. Some or all of the modes active in the ortho spectra are expected to be active in the spectra of the meta isomers. However, only three are observed. Two correspond to the bond deformation and ring stretch modes (ν_{22} and ν_7). These are measured to be ca. 520 and 1520 cm^{-1}, respectively. The frequencies obtained from the hot bands are for the ring deformation mode of the ions. The only other modes active in the meta spectra are ring deformation modes near 700 cm^{-1}, similar to that observed in the spectrum of **1a**$^-$.

Conclusion

We have measured and assigned the photoelectron spectra of the ortho, meta, and para isomers of fluoro-, chloro-, and bromo derivatives of benzyl anions. The electron affinities of the corresponding radicals have been determined. As expected, all the spectra are strikingly similar to the benzyl spectrum. The two active modes in the benzyl spectrum are active in all those reported here, although additional modes are active in the spectra of the lower symmetry species. The measured electron affinities are also employed in conjunction with gas-phase acidities and anion heats of formation from other studies to derive the 298 K bond energies and heats of formation of the halobenzyl radicals. We show that the electron affinity trends in the halobenzyl radicals are governed by the same parameters that govern the gas-phase acidities.

Supporting Information Available: Seven tables listing optimized geometries, bond lengths, bond angles, and vibrational frequencies for all the *o*-, *m*- and *p*-halobenzyl anions and radicals discussed in this paper, with all calculations carried out at the B3LYP/6-31+G* level of theory. This material is available free of charge via the Internet at http://pubs.acs.org.

References and Notes

(1) Selco, J. J.; Carrick, P. G. *J. Mol. Spectrosc.* **1989**, *137*, 13.

(2) Fukishima, M.; Obi, K. J. *J. Chem. Phys.* **1990**, *93*, 8488.

(3) Fukishima, M.; Obi, K. J. *J. Chem. Phys.* **1992**, *96*, 4224.

(4) Fukishima, M.; Obi, K. *Chem. Phys. Lett.* **1995**, *242*, 443.

(5) Fukishima, M.; Saito, K.; Obi, K. J. *J. Mol. Spectrosc.* **1996**, *180*, 389.

(6) Baskir, E. G.; Maltsev, A. K.; Korolev, V. A.; Khabashesku, V. N.; Nefedov, O. M. *Izv. Akad. Nauk SSSR, Ser. Khim.* **1993**, 1499.

(7) Eiden, G. C.; Weishaar, J. C. *J. Phys. Chem.* **1991**, *95*, 6194.

(8) Eiden, G. C.; Weinhold, F.; Weishaar, J. C. *J. Chem. Phys.* **1991**, *95*, 8665.

(9) Davico, G. E.; Bierbaum, V. M.; DePuy, C. H.; Ellison, G. B. *Int. J. Mass Spectrom. Ion Processes* **1995**, *156*, 109.

(10) Gunion, R. F.; Gilles, M. K.; Polak, M. L.; Lineberger, W. C. *Int. J. Mass Spectrom. Ion Processes* **1992**, *117*, 601.

(11) Carlton, T. R.; Thrush, B. A. *Chem. Phys. Lett.* **1986**, *125*, 547.

(12) Hiroshi, H.; Mori, K.; Shizuka, H.; Fukishima, M.; Obi, K. *Chem. Phys. Lett.* **1987**, *157*, 35.

(13) Fukishima, M.; Obi, K. *Chem. Phys. Lett.* **1996**, *248*, 269.

(14) Ervin, K. M.; Lineberger, W. C. Photoelectron Spectroscopy of Negative Ions. In *Advances in Gas Phase Ion Chemistry*; Adams, N. G., Babcock, L. M., Eds.; JAI Press: Greenwich, CT, 1992; Vol. 1, p 121.

(15) Leopold, D. G.; Murray, K. K.; Miller, A. E. S.; Lineberger, W. C. *J. Chem. Phys.* **1985**, *83*, 4849.

(16) Wenthold, P. G.; Squires, R. R. *J. Mass Spectrom.* **1995**, *30*, 17.

(17) Wenthold, P. G.; Wierschke, S. G.; Nash, J. J.; Squires, R. R. *J. Am. Chem. Soc.* **1994**, *116*, 7378.

(18) Wenthold, P. G.; Polak, M. L.; Lineberger, W. C. *J. Phys. Chem.* **1996**, *100*, 6920.

(19) Ervin, K. M.; Ho, J.; Lineberger, W. C. *J. Chem. Phys.* **1989**, *91*, 5974.

(20) Neumark, D. M.; Lykke, K. R.; Anderson, T.; Lineberger, W. C. *Phys. Rev. A* **1985**, *32*, 1890.

(21) Moore, C. E. *Atomic Energy Levels*; U.S. GPO Circular No. 467; Washington, 1952.

(22) Sharp, T. E.; Rosenstock, H. M. *J. Chem. Phys.* **1964**, *41*, 3453.

(23) Botter, R.; Dibeler, V. H.; Walker, J. A.; Rosenstock, H. M. *J. Chem. Phys.* **1966**, *44*, 1271.

(24) Duschinsky, F. *Acta Physicochim.* **1937**, *7*, 551.

(25) Cooper, J.; Zare, R. N. *J. Chem. Phys.* **1968**, *48*, 942.

(26) Cooper, J.; Zare, R. N. *J. Chem. Phys.* **1968**, *49*, 4252.

(27) Hall, J. L.; Siegel, M. W. *J. Chem. Phys.* **1968**, *48*, 943.

(28) Hanstorp, D.; Bengtsson, C.; Larson, D. J. *Phys. Rev. A* **1989**, *40*, 670.

(29) Gilles, M. K.; Polak, M. L.; Lineberger, W. C. *J. Chem. Phys.* **1992**, *96*, 8012.

(30) Gilles, M. K.; Ervin, K. M.; Ho, J.; Lineberger, W. C. *J. Phys. Chem.* **1992**, *96*, 1130.

(31) Wenthold, P. G.; Lineberger, W. C. *J. Am. Chem. Soc.* **1997**, *119*, 7772.

(32) Kato, S.; Lee, H. S.; Gareyev, R.; Wenthold, P. G.; Lineberger, W. C.; DePuy, C. H.; Bierbaum, V. M. *J. Am. Chem. Soc.* **1997**, *119*, 7863.

(33) Frisch, M. J.; Trucks, G. W.; Schlegal, H. B.; Gill, P. M. W.; Johnson, B. G.; Robb, M. A.; Cheeseman, J. R.; Kieth, T.; Petersson, G. A.; Montgomery, J. A.; Raghavachari, K.; Al-Laham, M. A.; Zakrewski, V. G.; Ortiz, J. V.; Foresman, J. B.; Cioslowski, J.; Stefanov, B. B.; Nanayakkara, A.; Challacombe, M.; Peng, C. Y.; Ayala, P. Y.; Chen, W.; Wong, M. W.; Andres, J. L.; Replogle, E. S.; Gomperts, R.; Martin, R. L.; Fox, D. J.; Binkley, J. S.; Defrees, D. J.; Baker, J.; Stewart, J. J. P.; Head-Gordon, M.; Gonzalez, C.; Pople, J. A. *Gaussian 94*, revision C.2; Gaussian, Inc.: Pittsburgh, PA, 1994.

(34) Berkowitz, J.; Ellison, G. B.; Gutman, D. *J. Phys. Chem.* **1994**, *98*, 2744.

(35) Bartmess, J. E. Negative Ion Energetics Data. In *NIST Chemistry WebBook, NIST Standard Reference Database Number 69*; Mallard, W. G., Linstrom, P. J., Eds.; National Institute of Standards and Technology: Gaithersburg, MD, 1999.

(36) Taft, R. W.; Topsom, R. D. benzyl37. In *Progress in Physical Organic Chemistry*; Taft, R. W., Ed.; John Wiley & Sons: New York, 1987; Vol. 16, pp 1–83.

(37) Tschumper, G. S.; Schaefer, H. F., III. *J. Chem. Phys.* **1997**, *107*, 2529.

(38) Rienstra-Kirocofe, J. C.; Graham, D. E.; Schaefer, H. F., III. *Mol. Phys.* **1998**, *94*, 767.

o-, *m*-, and *p*-Halobenzyl Anions

J. Phys. Chem. A, Vol. 103, No. 50, 1999 **10841**

(39) Wenthold, P. G. *Chem. Phys. Lett.* **1998**, *297*, 445.

(40) Wilson, E. B., Jr. *Phys. Rev.* **1934**, *45*, 706.

(41) Wenthold, P. G.; Kim, J. B.; Lineberger, W. C. *J. Am. Chem. Soc.* **1997**, *119*, 1354.

(42) Leopold, D. G.; Stevens-Miller, A. E.; Lineberger, W. C. *J. Am. Chem. Soc.* **1986**, *108*, 1379.

(43) Wenthold, P. G.; Squires, R. R.; Lineberger, W. C. *J. Am. Chem. Soc.* **1998**, *120*, 5279.

(44) Jacox, M. E. *J. Phys. Chem. Ref. Data* **1990**, *19*, 1500.

(45) Chen, P. Photoelectron spectroscopy of reactive intermediates. In *Unimolecular and Bimolecular Reaction Dynamics*; Ng, C. Y., Baer, T., Powis, I., Eds.; John Wiley & Sons: New York, 1994.